Spontaneous-Emission Rate in Microcavities: Application to Two-Dimensional Photonic Crystals

C. Shen, K. Michielsen, and H. De Raedt*

Department of Applied Physics, Materials Science Centre, University of Groningen, Nijenborgh 4, NL-9747 AG Groningen, The Netherlands

(Received 24 October 2005; published 29 March 2006)

We present a simple, efficient procedure to compute the spontaneous-emission rate from short-time finite-difference time-domain (FDTD) data of the electromagnetic field energy in microcavities of arbitrary geometry. As an illustration, we apply this procedure to two-dimensional photonic crystals. For comparison, we calculate the local radiative density of states employing an unconditionally stable FDTD method, that is without solving the eigenvalue problem and integrating over the (first) Brillouin zone. We demonstrate that both methods yield the same predictions about the enhancement or suppression of the spontaneous-emission rate by photonic crystals.

DOI: 10.1103/PhysRevLett.96.120401 PACS numbers: 03.50.De, 42.25.Gy, 42.60.Da, 42.70.Qs

Spontaneous emission of light is a widely studied phenomenon, both due to its importance in the fundamental understanding of light-matter interactions and in the applications, such as, for example, transistors, optical switches, microlasers, solar cells, etc., which depend on it. Already in 1946, it was noticed that spontaneous emission can be controlled with cavity structures [1]. Theoretically, the spontaneous-emission rate can be obtained from Fermi's golden rule containing the local radiative density of states (LRDOS) [2]. For relatively simple cavity structures, the modification of the spontaneous-emission rate can be calculated analytically using either a classical [3–8] or a quantum mechanical approach [9]. It has been shown that the classical and quantum mechanical results for the spontaneous emission are equivalent [3,5,7,8]. This equivalence allows the calculation of the spontaneous-emission rate [10–12], the external quantum efficiency [12], and the spontaneous-emission factor [12,13] in a microcavity of arbitrary geometry, using a finite-difference time-domain (FDTD) algorithm [14].

Control of spontaneous emission is also one of the main applications of photonic crystals (PhCs) [15–17]. It was suggested that PhCs with a complete photonic band gap (PBG) allow complete inhibition of spontaneous emission for frequencies deep inside the PBG [15]. Also PBG materials that do not possess complete PBGs but pseudogaps are of interest since they can allow for a substantially suppressed spontaneous emission. Recent experiments on the control of spontaneously emitted light in PhCs have demonstrated the suppression of light emission caused by the effect of the PBG [16].

In this Letter, we present a simple procedure to determine the spontaneous-emission rate from short-time FDTD data of the EM field energy. We validate this procedure by computing the LRDOS of two-dimensional (2D) PhCs, employing an unconditionally stable FDTD method [14,18]. Although this computation is more expensive than the procedure based on the EM field energy data, this FDTD based method does not require a solution of the eigenvalue problem nor integrations over the (first) Brillouin zone (FBZ).

We write the time-dependent Maxwell equations (TDME) for the EM fields in linear, isotropic, lossless, nondispersive dielectric materials without electric charges and magnetic current sources as [18]

$$\frac{\partial}{\partial t}\psi(t) = H\psi(t) - S(t), \tag{1}$$

where H denotes the operator

$$\begin{pmatrix} 0 & -\frac{1}{\sqrt{\mu(\mathbf{r})}}\nabla\times\frac{1}{\sqrt{\epsilon(\mathbf{r})}} \\ \frac{1}{\sqrt{\epsilon(\mathbf{r})}}\nabla\times\frac{1}{\sqrt{\mu(\mathbf{r})}} & 0 \end{pmatrix}, \tag{2}$$

$S(t) = (0, \mathbf{J}(\mathbf{r}, t)/\sqrt{\epsilon(\mathbf{r})})^T$ denotes the source term, and $\psi(t) = (\sqrt{\mu(\mathbf{r})}\mathbf{H}(\mathbf{r}, t), \sqrt{\epsilon(\mathbf{r})}\mathbf{E}(\mathbf{r}, t))^T$. Here $\epsilon(\mathbf{r})$, $\mu(\mathbf{r})$, $\mathbf{J}(\mathbf{r}, t)$ denote the electrical permittivity, the magnetic permeability, and an electric current source, respectively, and $\mathbf{r} = (x, y, z)^T$ denotes the position vector of a point in space.

By construction,

$$\langle\psi(t)|\psi(t)\rangle = \int_V [\epsilon(\mathbf{r})\mathbf{E}^2(\mathbf{r}, t) + \mu(\mathbf{r})\mathbf{H}^2(\mathbf{r}, t)]d\mathbf{r}, \tag{3}$$

relating the length of $\psi(t)$ to the energy density $w(\mathbf{r}, t) = \epsilon(\mathbf{r})\mathbf{E}^2(\mathbf{r}, t) + \mu(\mathbf{r})\mathbf{H}^2(\mathbf{r}, t)$ of the EM fields. Here V denotes the volume of the enclosing box. The energy emitted by the point source can thus be defined as $U(t) = \langle\psi(t)|\psi(t)\rangle$. The emission rate can be obtained by differentiation of $U(t)$: $P(t) = \partial U(t)/\partial t$.

As mentioned earlier, the emission properties can also be investigated by calculating the LRDOS. Here we demonstrate that there is a simple relation between the emitted energy and the LRDOS. The formal solution of Eq. (1) is given by

$$\psi(t) = e^{tH}\psi(0) - \int_0^t e^{(t-u)H}S(u)du. \tag{4}$$

We assume that the electric current density of a unit point source located at $\mathbf{r} = \mathbf{r_0}$ is given by

$$\mathbf{J}(\mathbf{r}, t) = \mathbf{n}\theta(t)\delta(\mathbf{r} - \mathbf{r_0})\sin\Omega t, \tag{5}$$

where Ω is the angular frequency of the source and $\mathbf{n}$ defines the direction of the electric current. As indicated by the step function $\theta(t)$ in Eq. (5), the source is turned on at $t = 0$. Making use of Eqs. (4) and (5) and assuming that $\psi(\mathbf{r}, t = 0) = 0$, we find

$$\begin{aligned} U(t) &= \langle\psi(t)|\psi(t)\rangle \\ &= \frac{1}{\epsilon(\mathbf{r}_0)}\int_0^t\int_0^t \langle\mathbf{S}_0|e^{(u'-u)H}\mathbf{S}_0\rangle \sin\Omega u \sin\Omega u' du du', \\ &= \frac{1}{2\pi}\int_{-\infty}^{+\infty}\int_0^t\int_0^t N_{\mathrm{rad}}(\mathbf{S}_0, \mathbf{n}, \omega)\cos\omega(u' - u) \\ &\quad \times \sin\Omega u \sin\Omega u' du du' d\omega, \end{aligned} \tag{6}$$

where $\mathbf{S}_0 = (0, \hat{\mathbf{S}}_0)$ and $\langle\mathbf{r}|\hat{\mathbf{S}}_0\rangle = \mathbf{n}\delta(\mathbf{r} - \mathbf{r}_0)$. The LRDOS is defined by $N_{\mathrm{rad}}(\mathbf{S}_0, \mathbf{n}, \omega) = \epsilon(\mathbf{r}_0)^{-1}N(\mathbf{S}_0, \mathbf{n}, \omega)$, where

$$N(\mathbf{S}_0, \mathbf{n}, \omega) \equiv \int_{-\infty}^{+\infty} e^{i\omega t}\langle\mathbf{S}_0|e^{tH}\mathbf{S}_0\rangle dt, \tag{7}$$

denotes the local density of states (LDOS) for frequency ω and direction $\mathbf{n}$ at the position $\mathbf{r}_0$. We carry out the time integration in Eq. (6) to obtain

$$\begin{aligned} U(t) = \frac{1}{\pi}\int_{-\infty}^{+\infty} N_{\mathrm{rad}}(\mathbf{S}_0, \mathbf{n}, \omega)\Bigg[&\frac{\sin^2 t(\omega - \Omega)/2}{(\omega - \Omega)^2} \\ &- \frac{\sin t(\omega - \Omega)/2}{\omega - \Omega}\,\frac{\sin t(\omega + \Omega)/2}{\omega + \Omega}\cos t\Omega\Bigg] d\omega. \end{aligned} \tag{8}$$

In the limit $t \to \infty$ the contribution of the second term in Eq. (8) vanishes, yielding for the emission rate

$$\begin{aligned} \lim_{t\to\infty} P(t) &= \lim_{t\to\infty} \partial U(t)/\partial t, \\ &= \lim_{t\to\infty}\int_{-\infty}^{+\infty} N_{\mathrm{rad}}(\mathbf{S}_0, \mathbf{n}, \omega)\frac{\sin t(\omega - \Omega)}{2\pi(\omega - \Omega)} d\omega, \\ &= N_{\mathrm{rad}}(\mathbf{S}_0, \mathbf{n}, \Omega)/2, \end{aligned} \tag{9}$$

which, apart from some constants, agrees with Eq. (26) in Ref. [7] and with the expression obtained by using Fermi's golden rule [19].

For microcavities of arbitrary geometry $U(t)$ is most easily calculated by solving the TDME by means of an FDTD method [14]. We employ an algorithm that, in the absence of external currents, conserves the energy exactly [14,18]. This property ensures that the time dependence of $U(t)$ is due to the presence of the source only. In our numerical work, we use square simulation areas completely filled with the PhC and having boundaries that are perfect reflecting conductors. We measure distances in units of the wavelength λ of light in vacuum. Time and frequency are then expressed in units of λ/c and c/λ, respectively, where c denotes the velocity of light in vacuum. For PhCs with lattice constant a, $f = \omega a/(2\pi c)$ is the dimensionless frequency.

We study the emission properties of a point source embedded in a 2D PhC. The PhC consists of a triangular lattice of air holes drilled in a dielectric material with $\epsilon = 13$ and $\mu = 1$. We study two cases, the holes having a diameter $d = 0.80a$ and $d = 0.96a$, respectively. For reference, we use the MIT Photonic-Bands (MPB) package [20] to compute the photonic band structure diagram for the TM mode. The results are shown in Fig. 1. For $d = 0.80a$, no gap is observed. For $d = 0.96a$ there is a gap extending from $f = 0.43$ to $f = 0.52$.

To compute the emitted energy, we put a point source with a current density specified by Eq. (5) at different locations $\mathbf{r}_0$ near the center of the simulation area. The locations are chosen such that the source is located at one of the E_z points of the 2D Yee grid (TM mode). The emitted energy $U(t)$ is trivially obtained from the solution for the EM fields, see Eq. (3). In order to have a reference value for the emitted energy, we first compute $U(t)$ for a point source located in the middle of a square area completely filled with air. In what follows, we refer to this setup as the empty area. The result is shown in Fig. 2 (crosses). The slope of the line through the data for $t \leq 20$ gives a measure for the emission rate (up to a scaling factor). For larger times the data deviate from a straight line. This is due to reflections at the boundaries of the simulation area. The solid symbols in Fig. 2 denote the results for a point source embedded in the PhC with $d = 0.80a$. We show three results for a source emitting light with a frequency $f = 0.30$. If the source is located in the center of a hole (solid squares) the emitted energy is very small and almost constant as a function of time. Hence, light emission is strongly suppressed and for all practical purposes inhibited. If we move the source away from the center of the hole, but so that it is still located in the air region (solid triangles), light emission is enhanced compared to the case for which the source was placed in the center of the hole (solid squares), but strongly suppressed compared to the empty area case (crosses). Placing the source in a region with $\epsilon = 13$ leads to an

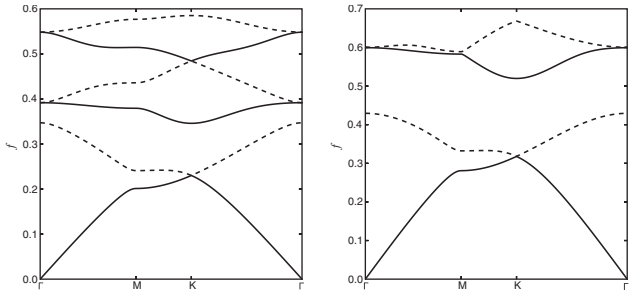

FIG. 1. Photonic band structure diagram of TM modes for a triangular lattice of air holes drilled in a dielectric medium ($\epsilon = 13$, $\mu = 1$). The holes have a diameter $d = 0.80a$ (left) and $d = 0.96a$ (right), where a denotes the lattice constant.

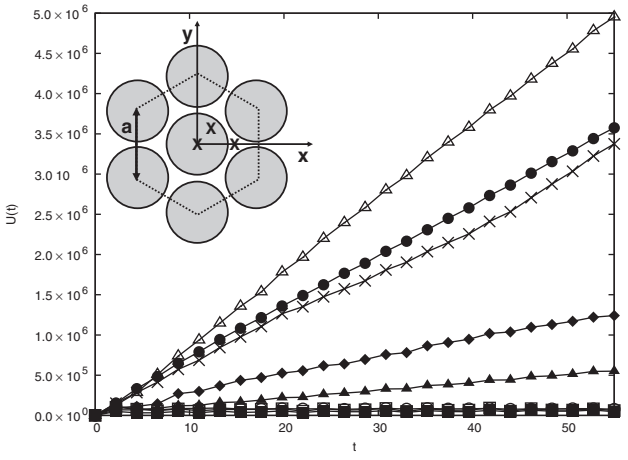

FIG. 2. Emitted energy U as a function of time t for a point source embedded in air (crosses) and for a point source located at position $\mathbf{r}_0$ in a 2D triangular-lattice PhC. The inset shows the triangular-lattice network with spacing a in real space. The crosses indicate the source positions $\mathbf{r}_0$. Solid symbols: $d = 0.80a$, open symbols: $d = 0.96a$. Solid squares: $\mathbf{r}_0 = (0, 0)$, $f = 0.30$; solid triangles: $\mathbf{r}_0 = a(0.20, 0.23)$, $f = 0.30$; solid circles: $\mathbf{r}_0 = a(\sqrt{3}/3, 0)$, $f = 0.30$; solid diamonds: $\mathbf{r}_0 = (0, 0)$, $f = 0.53$; open squares: $\mathbf{r}_0 = (0, 0)$, $f = 0.48$; open circles: $\mathbf{r}_0 = a(\sqrt{3}/3, 0)$, $f = 0.48$; open triangles: $\mathbf{r}_0 = (0, 0)$, $f = 0.56$.

emission enhancement (solid circles) compared to the empty area case. Changing the frequency to $f = 0.53$ and putting the source in the center of a hole also leads to a suppression of the light emission (solid diamonds), but not to an inhibition of the emission, as in the case of $f = 0.3$. From these results, it can be concluded that the emission rate strongly depends on the location of the source and on the frequency of the emitted light: emission enhancement as well as emission suppression can be observed. Even if the PhC has no PBG, the emission of a point source can be almost completely suppressed [2].

Figure 2 also shows the results of the energy emitted by a point source embedded in the PhC with $d = 0.96a$, a PhC having a PBG. For $f = 0.48$, a frequency inside the PBG, and sources located in the center of a hole (open squares) or in the dielectric material (open circles), light emission is inhibited for all practical purposes. Note that the values for $U(t)$ for these two cases are comparable to the value of $U(t)$ for the case of a source emitting light with a frequency $f = 0.3$ and located in the center of a hole in the PhC with $d = 0.80a$. Increasing the frequency of the light emitted by a source, located at the center of a hole, to $f = 0.56$ (open triangles) leads to a strong emission enhancement compared to the empty area case.

We validate the conclusions based on the behavior of the results for $U(t)$ by computing the LRDOS. We use the following procedure: we first set the EM fields at the point $\mathbf{r}_0$ on the 2D Yee grid so that $E_z(\mathbf{r}_0, t) = 1$ and so that all other (components of the) EM fields are zero at all other points of the grid. We then solve the TDME and store the values of $f(t) = \epsilon(\mathbf{r}_0)^{-1}\langle \mathbf{S}_0 | e^{tH} \mathbf{S}_0 \rangle$. The (fast) Fourier transform of $f(t)$ then yields the LRDOS. By using an unconditionally stable algorithm [14,18], we do not have to solve the eigenvalue problem for H [21]. This is an important advantage over methods that compute the L(R)DOS by integrating the modulus of the electric field in the FBZ. Not only does the diagonalization require a lot of computer time, also all points of the entire FBZ should be included in the calculation of the L(R)DOS [22]. As pointed out in Ref. [22], this integral was often performed incorrectly within an irreducible FBZ [23] by using a linear tetrahedron method.

Figures 3 and 4 show the results for the LRDOS for the same source positions as the ones used to obtain the results depicted in Fig. 2. Figure 3 shows the LRDOS for sources embedded the PhC with $d = 0.80a$. If the source is located in the center of a hole [see Fig. 3(a)], then the LRDOS shows a small gap around $f = 0.30$. In this frequency range there are no EM modes. Hence, light with a frequency $f = 0.30$ emitted by a source positioned in the center of a hole cannot propagate into the PhC. Note, however, that the PhC has no PBG and hence the DOS has no gaps around $f = 0.30$. Increasing the frequency of the source to, for example, $f = 0.53$ allows the light to propagate through the system. Moving the source away from the center of the hole, but in a way that it is still located in the air region, results in an increase of the density of states around $f = 0.30$ [see Fig. 3(b)]. Although the LRDOS is still rather small at $f = 0.30$, light can now propagate into the PhC. From Fig. 3(c) it can be seen that placing the source in a region with $\epsilon = 13$ leads to a further increase of the LRDOS around $f = 0.3$. Comparing the results of Fig. 2 with the results of Fig. 3 indicates that the number of modes at a given frequency gives a rough quantitative measure of the emission rate. Figure 4 depicts the LRDOS for the case $d = 0.96a$. For frequencies inside the PBG, no modes are available, inde-

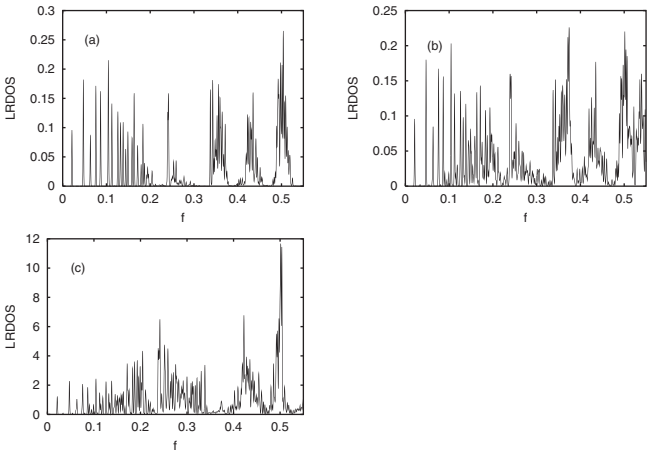

FIG. 3. LRDOS for various source locations $\mathbf{r}_0$ in the PhC with $d = 0.80a$. (a) $\mathbf{r}_0 = (0, 0)$; (b) $\mathbf{r}_0 = a(0.20, 0.23)$; (c) $\mathbf{r}_0 = a(\sqrt{3}/3, 0)$.

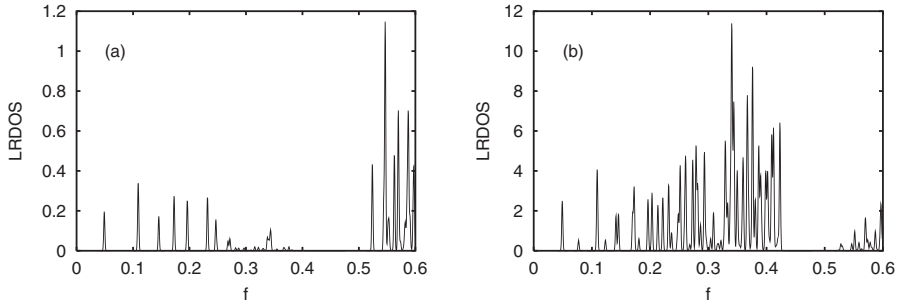

FIG. 4. LRDOS for various source locations $\mathbf{r}_0$ in the PhC with $d = 0.96a$. (a) $\mathbf{r}_0 = (0, 0)$; (b) $\mathbf{r}_0 = a(\sqrt{3}/3, 0)$.

pendent of the position of the source. Hence, for $f = 0.48$ emission is inhibited, as was also concluded from Fig. 2. For $f = 0.56$, a frequency in a passband, no gaps in the LRDOS are seen for source positions in a hole.

In summary, we have presented a simple, efficient procedure to extract the spontaneous-emission rate from short-time FDTD data of the EM field energy in microcavities of arbitrary geometry and demonstrated its validity by comparison with L(R)DOS calculations for PhCs.

This work is part of the research programme ''Waves in Complex Media'' from the ''Stichting voor Fundamenteel Onderzoek der Materie''(FOM) which is financially supported by the ''Nederlandse Organisatie voor Wetenschappelijk Onderzoek''(NWO).

*Electronic address: h.a.de.raedt@rug.nl

[1] E. M. Purcell, Phys. Rev. **69**, 681 (1946).
[2] R. Sprik, B. A. van Tiggelen, and A. Lagendijk, Europhys. Lett. **35**, 265 (1996).
[3] H. Morawitz, Phys. Rev. **187**, 1792 (1969).
[4] K. H. Tews, J. Lumin. **9**, 223 (1974).
[5] H. Chew, Phys. Rev. A **38**, 3410 (1988).
[6] J. P. Dowling, M. Scully, and F. DeMartini, Opt. Commun. **82**, 415 (1991).
[7] J. P. Dowling and C. M. Bowden, Phys. Rev. A **46**, 612 (1992).
[8] H. Rigneault and S. Monneret, Phys. Rev. A **54**, 2356 (1996).
[9] G. S. Agarwal, Phys. Rev. A **12**, 1475 (1975); A. O. Barut and J. P. Dowling, Phys. Rev. A **36**, 649 (1987); X.-P. Feng and K. Ujihara, Phys. Rev. A **41**, 2668 (1990); R. J. Glauber and M. Lewenstein, Phys. Rev. A **43**, 467 (1991); G. Björk *et al.*, Phys. Rev. A **44**, 669 (1991); S. M. Barnett, B. Huttner, and R. Loudon, Phys. Rev. Lett. **68**, 3698 (1992); H. Khosravi and R. Loudon, Proc. R. Soc. London, Ser. A **436**, 373 (1992); K. Kakazu and Y. S. Kim, Phys. Rev. A **50**, 1830 (1994); N. Koide and K. Ujihara, Opt. Commun. **111**, 381 (1994); W. Zakowicz and A. Bledowski, Phys. Rev. A **52**, 1640 (1995); S. M. Barnett and R. Loudon, Phys. Rev. Lett. **77**, 2444 (1996).
[10] Y. Xu *et al.*, J. Opt. Soc. Am. B **16**, 465 (1999).
[11] J.-K. Hwang, H.-Y. Ryu, and Y.-H. Lee, Phys. Rev. B **60**, 4688 (1999).
[12] Y. Xu, R. K. Lee, and A. Yariv, Phys. Rev. A **61**, 033807 (2000).
[13] J. Vučković *et al.*, IEEE J. Quantum Electron. **35**, 1168 (1999).
[14] A. Taflove and S. C. Hagness, *Computational Electrodynamics: The Finite-Difference Time-Domain Method* (Artech House, MA, USA, 2005), 3rd ed.
[15] E. Yablonovitch, Phys. Rev. Lett. **58**, 2059 (1987).
[16] P. Lodahl *et al.*, Nature (London) **430**, 654 (2004); S. Ogawa *et al.*, Science **305**, 227 (2004); M. Fujita *et al.*, Science **308**, 1296 (2005).
[17] I. S. Nikolaev, P. Lodahl, and W. L. Vos, Phys. Rev. A **71**, 053813 (2005); S. Richter *et al.*, Appl. Phys. Lett. **87**, 142107 (2005); A. Kress *et al.*, Phys. Rev. B **71**, 241304(R) (2005); D. Englund *et al.*, Phys. Rev. Lett. **95**, 013904 (2005); A. Badolato *et al.*, Science **308**, 1158 (2005).
[18] J. S. Kole, M. T. Figge, and H. De Raedt, Phys. Rev. E **64**, 066705 (2001).
[19] L. E. Ballentine, *Quantum Mechanics: A Modern Development* (World Scientific, Singapore, 2003).
[20] S. G. Johnson and J. D. Joannopoulos, Opt. Express **8**, 173 (2001).
[21] A. Hams and H. De Raedt, Phys. Rev. E **62**, 4365 (2000).
[22] R. Wang *et al.*, Phys. Rev. B **67**, 155114 (2003).
[23] T. Suzuki and P. K. L. Yu, J. Opt. Soc. Am. B **12**, 570 (1995); K. Busch and S. John, Phys. Rev. E **58**, 3896 (1998); Z. Y. Li, L.-L. Lin, and Z.-Q. Zhang, Phys. Rev. Lett. **84**, 4341 (2000); Z. Y. Li and Y. Xia, Phys. Rev. A **63**, 043817 (2001).